# Novel Ternary Composite Electrolytes: Li Ion Conducting Ionic Liquids in Silica Glass

Thomas Echelmeyer, Hinrich Wilhelm Meyer, and Leo van Wüllen*

*Institut für Physikalische Chemie, Westfälische Wilhelms-Universität Münster, Corrensstrasse 30, 48149 Münster, Germany*

*Received February 20, 2009. Revised Manuscript Received April 2, 2009*

In this contribution, we report on a novel composite solid electrolyte material, $SiO_2$/[BMIM]$BF_4$/LiTf ([BMIM]$BF_4$ = 1-butyl-3-methylimidazolium tetrafluoroborate, LiTf = lithium trifluoromethanesulfonate), prepared via a one-pot sol−gel synthesis route, in which the amorphous $SiO_2$ glass network provides the mechanical stability and the ionic liquid/Li salt part the high ionic conductivity ($0.5 \times 10^{-2}$ S cm$^{-1}$ at 298 K). The mobility of the ionic liquid and Li salt confined within the pores of the fully condensed $SiO_2$ network is found to increase with the [BMIM]$BF_4$/LiTf ratio, exhibiting an almost liquidlike mobility, as evidenced by multinuclear solid-state NMR, pulsed-field-gradient solid-state NMR, and impedance spectroscopy.

## Introduction

Due to the ever-increasing demand for low-weight Li batteries for mobile electronics, the search for an ideal solid ion conductor for use as solid electrolyte in battery applications is still an important facet of materials science.[1−4] Apart from desirable properties such as a high chemical resistance, environmental compatibility and low weight, the mechanical stability and ionic conductivity for the transported Li ions in combination with a vanishing electronic contribution constitute the key requirements that have to be met by the ideal lithium ion conducting solid electrolyte. Although recent years have witnessed considerable progress in the search for polymer[3−5] and crystalline[6−9] Li ion conducting solid electrolytes, the optimization of the ionic conductivity without compromising too much on the other properties (mechanical strength, environmental compatibility, etc.) still poses a serious challenge. In many cases, the optimization of the mechanical stability or the ionic conductivity entails an unacceptable deterioration of the other. Thus, a cross-linking of a polymer increases the mechanical stability at the cost of a decrease in the ionic conductivity; the addition of plasticizers, on the other hand, amends the amorphicity and hence the ionic conductivity of the polymer, but only at the cost of an impairment of the mechanical stability.

A promising path to overcome this dilemma and consequently toward better performing solid electrolytes may be opened by a complete decoupling of the mechanical and the ion conducting properties. Such a system would comprise an inert solid host material that provides good mechanical stability, in which a second phase (solid or liquid) displaying high ionic conductivity is confined. Possible candidates for the solid host material include stabilized polymers or inorganic glasses; Li salts dissolved in an ionic liquid (IL) may serve as the ion conducting phase. The first reports about the combination of a polymer host with a Li salt/ionic liquid as the conducting phase exhibiting room temperature ionic conductivities >$10^{-4}$ S cm$^{-1}$ have appeared in the literature;[10−13] however, the mechanical performance of these materials still seems to be rather limited. In this respect, composite systems of a silica glass, an ionic liquid, and a Li salt might evolve as an attractive alternative to the established routes. As has been shown by several authors, the system IL/$SiO_2$, synthesized via a nonaqueous sol−gel route, forms stable solid membranes.[14−19] In these solid materials, the ionic liquid exhibits an almost fluidlike dynamic, although being confined within the silica network.[20,21] Consequently, these systems

* To whom correspondence should be addressed. Tel: +492518323445. Fax: +492518323404. E-mail: wullen@uni-muenster.de.

(1) Bruce, P. G.; Scrosati, B.; Tarascon, J.-M. *Angew. Chem., Int. Ed.* **2008**, *47*, 2930.
(2) Patil, A.; Patil, V.; Shin, D. W.; Choi, J.-W.; Paik, D.-S.; Yoon, S.-J. *Mater. Res. Bull.* **2008**, *43*, 913.
(3) Stephan, A. M.; Nahm, K. S. *Polymer* **2006**, *47*, 5952.
(4) Agrawal, R. C.; Pandey, G. P. *J. Phys. D* **2008**, *41*, 22301.
(5) Bruce, P. G. *Solid State Ionics* **2008**, *179*, 752.
(6) Kanno, R.; Murayama, M. *J. Electrochem. Soc.* **2001**, *148*, A742.
(7) Murayama, M.; Sonoyama, N.; Yamada, A.; Kanno, R. *Solid State Ionics* **2004**, *170*, 173.
(8) Deiseroth, H. J.; Kong, S. T.; Eckert, H.; Vannahme, J.; Reiner, C.; Zaiss, T.; Schlosser, M. *Angew. Chem., Int. Ed.* **2008**, *47*, 755.
(9) Murugan, R.; Thangadurai, V.; Weppner, W. *Angew. Chem., Int. Ed.* **2007**, *46*, 7778.
(10) Shin, J. H.; Henderson, W. A.; Passerini, S. *J. Electrochem. Soc.* **2005**, *152*, A978.
(11) Rymarczyk, J.; Carewska, M.; Appetecchi, G. B.; Zane, D.; Alessandrini, F.; Passerini, S. *Eur. Polym. J.* **2008**, *44*, 2153.
(12) Mizumo, T. *Kobunshi Ronbunshu* **2008**, *65*, 516.
(13) Rupp, B.; Schmuck, M.; Balducci, A.; Winter, M.; Kern, W. *Eur. Polym. J.* **2008**, *44*, 2986.
(14) Lunstroot, K.; Driesen, K.; Nockermann, P.; Gorller-Walrand, C.; Binnemans, K.; Bellayer, S.; Le Bideau, J.; Vioux, A. *Chem. Mater.* **2006**, *18*, 5711.
(15) Zhang, L.; Zhang, Q.; Li, J. H. *J. Electroanal. Chem.* **2007**, *603*, 243.
(16) Neouze, M. A.; Le Bideau, J.; Leroux, F.; Vioux, A. *Chem. Commun.* **2005**, 1082.
(17) Neouze, M. A.; Le Bideau, J.; Vioux, A. *Prog. Solid State Chem.* **2005**, *33*, 217.
(18) Jacob, D. S.; Gedanken, A. *J. Am. Ceram. Soc.* **2008**, *91*, 3024.
(19) Jacob, D. S.; Joseph, A.; Mallenahalli, S. P.; Shanmugam, S.; Makhluf, S.; Calderon-Moreno, J.; Koltypin, Y.; Gedanken, A. *Angew. Chem., Int. Ed.* **2005**, *44*, 6560.

10.1021/cm9005184 CCC: $40.75 
Published on Web 04/30/2009

**Table 1. Batch Compositions (in relative molar ratios) and Solid-State NMR Parameters for the Samples Investigated in This Work**

| | | | | | | | | | | |
|---|---|---|---|---|---|---|---|---|---|---|
| | | | | | | | $^{19}$F | | | |
| | sample compositions | | | | $^{7}$Li | | | Tf | | $BF_4$ |
| glass sample | TEOS | LiTf | [BMIM]$BF_4$ | HCOOH | $\delta_{iso}$/ppm | $\nu_Q$/kHz | fwhm/Hz | $\delta_{iso}$/ppm | $\Delta\sigma$/ppm | $\delta_{iso}$/ppm |
| [BMIM]$BF_4$ | 0 | 0 | 1 | 0 | – | – | | – | – | −149.9 |
| LiTf | 0 | 1 | 0 | 0 | −1.4 | 65 | 4300 | −79.3 | 72 | – |
| ig_0 | 1 | 0.5 | 0 | 8.8 | – | – | – | – | – | – |
| ig_1 | 1 | 0.5 | 0.5 | 8.8 | −1.1 | 70 | 590 | −80.0 | 68 | −153.2 |
| ig_2 | 1 | 0.5 | 1 | 8.8 | −1.3 | – | 154 | −79.4 | – | −152.0 |
| ig_3 | 1 | 0.5 | 2 | 8.8 | −1.3 | – | 113 | −79.3 | – | −151.2 |
| ig_3.2 | 1 | 0.5 | 2 | 8.8 | −1.4 | – | 126 | −79.3 | – | −152.2 |

were advertised as promising materials for electrolytes in fuel cells or dye-sensitized solar cells.[17,20] However, to the best of our knowledge, no report has been given to date about the performance of $SiO_2$/IL/Li salt composites as Li ion conductors, although we acknowledge that this possible application has been mentioned by Le Bideau and Vioux.[16,17,20]

Here we report the first experimental data on a ternary composite in which an ionic liquid, 1-butyl-3-methylimidazolium tetrafluoroborate ([BMIM]$BF_4$), together with a lithium salt, lithium tetrafluoromethane sulfonate (LiTf), is confined within a $SiO_2$ glass synthesized via a nonaqueous sol−gel process employing tetraethoxysilane (TEOS) as the source for silicon and formic acid as the solvent.[22] The network structure of the silica network and the dynamic state of the various anions and cations confined within the silica network are analyzed by employing solid-state NMR techniques. The mobility of the Li cations and triflate and tetrafluoroborate anions are found to increase in synchrony with the [BMIM]$BF_4$/LiTf ratio. For the sample with the highest [BMIM]$BF_4$/LiTf ratio, an almost liquidlike dynamic behavior is observed already at temperatures below ambient, entailing a very high ionic conductivity of $0.5 \times 10^{-2}$ S cm$^{-1}$ at 298 K.

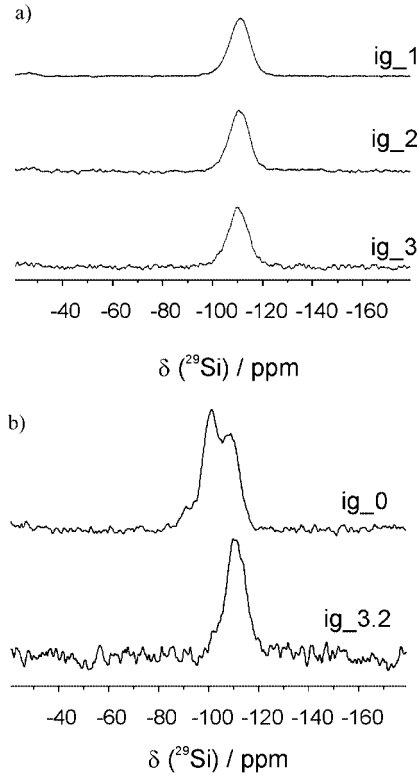


**Figure 1.** (a) $^{29}$Si-MAS NMR spectra for the ionogel-glass samples studied in this work. All spectra were recorded at room temperature. (b) comparison of the $^{29}$Si MAS NMR spectra for samples ig_3.2 ($SiO_2$/LiTf/[BMIM]$BF_4$ = 1:0.5:2) and the IL-free sample ig_0. Note the exclusive presence of the signal at −110 ppm, indicating a fully condensed network for sample ig_3.2, whereas the appearance of three signals at −91 ppm ($Q^2$), −102 ppm ($Q^3$), and −110 ppm ($Q^4$) for the ionic-liquid-free reference sample shows that the gel-to-glass conversion is incomplete in this case. Experimental details: $\nu_{MAS}$ = 5 kHz; $\pi/2$-pulse length, 6 $\mu$s; repetition time, 60 s; spectral width, 25 kHz. An exponential line broadening of 50 Hz was employed to smooth the data.

## Experimental Section

**Synthesis.** Lithium trifluoromethanesulfonate (LiTf; Aldrich, 99.995%) was dried at 120 °C in vacuo prior to use. The ion-conducting ionogel-glasses were prepared by employing a

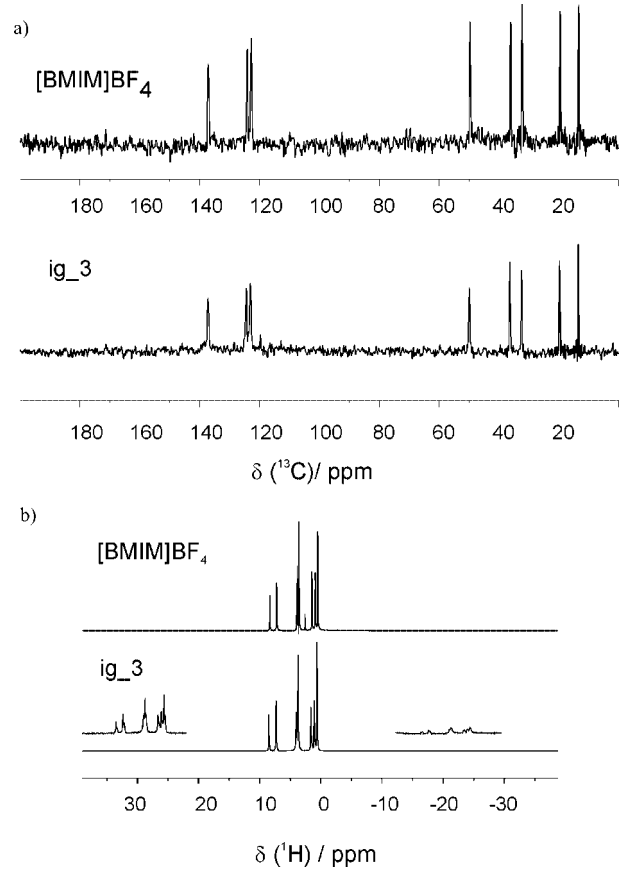


**Figure 2.** $^{13}$C (a) and $^{1}$H MAS NMR spectra (b) for the pristine ionic liquid [BMIM]$BF_4$ (top) and the ionogel-glass ig_3 (bottom). The insets show the spinning sidebands in a magnified (×40) view. Experimental details: $\nu_{MAS}$ = 10 kHz; $\pi/2$-pulse length, 3−4 $\mu$s ($^{13}$C), 7.25 $\mu$s ($^{1}$H); repetition time, 60 s ($^{13}$C), 5−15 s ($^{1}$H). An exponential line broadening of 15 Hz ($^{13}$C) and 1 Hz ($^{1}$H) was used to smooth the data.

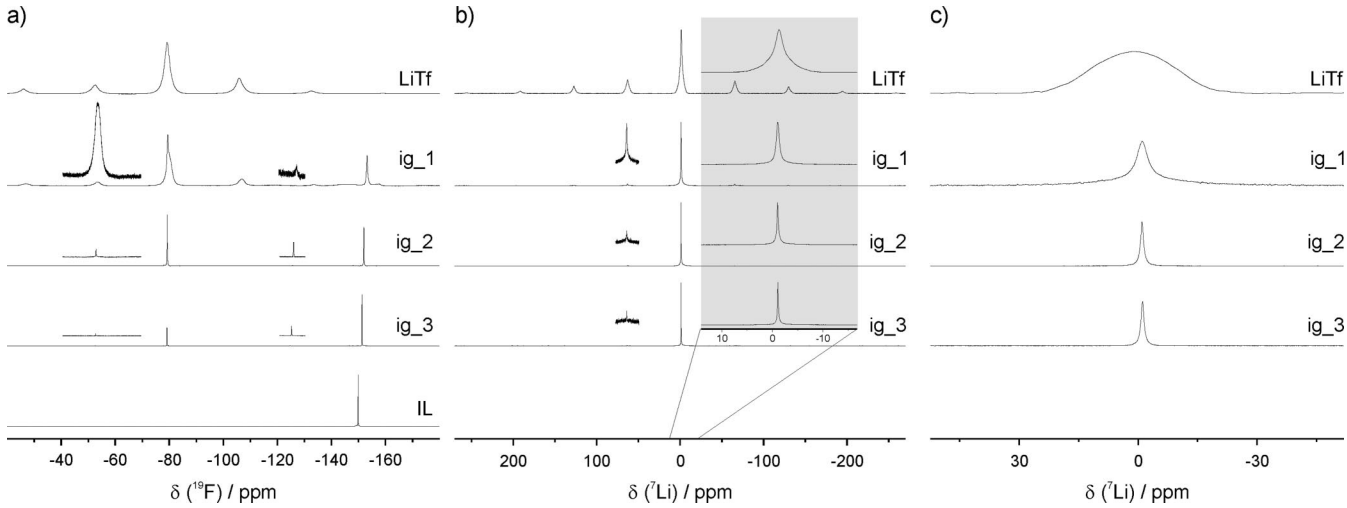


**Figure 3.** $^{19}$F-MAS (a), $^{7}$Li-MAS (b), and static $^{7}$Li spin echo NMR (c) spectra for the studied ionogel-glasses. The spectra for pristine LiTf are incorporated for comparison. An expanded view of some spinning sidebands ($y$-scale × 20) is shown in the insets. Experimental details: $\nu_{MAS}$ = 10 kHz; $\pi$/2-pulse lengths = 2 $\mu$s ($^{19}$F), 5 $\mu$s ($^{7}$Li); repetition time, 2−15 s ($^{19}$F), 5−90 s ($^{7}$Li). An exponential line broadening of 1 Hz ($^{19}$F), 5 Hz ($^{7}$Li-MAS), and 25 Hz ($^{7}$Li static) was used to smooth the data.

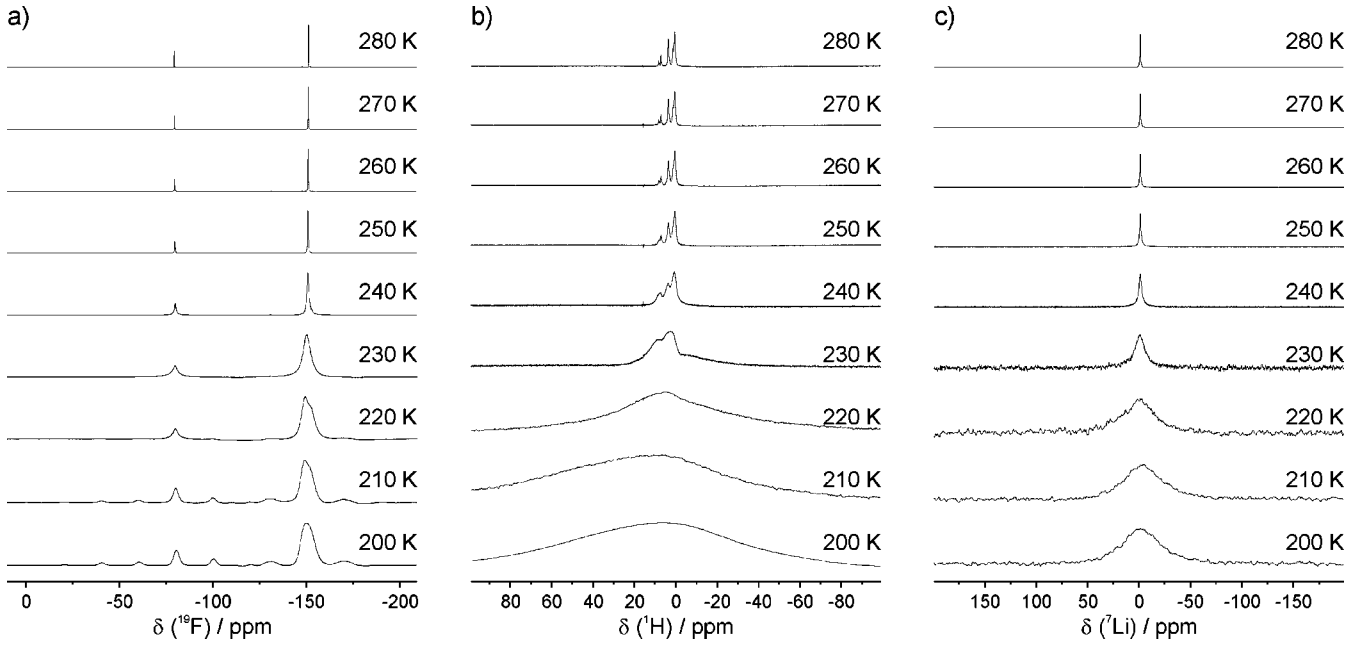


**Figure 4.** $^{19}$F MAS (a), static $^{1}$H (b), and static $^{7}$Li spin echo NMR spectra (c) for ionogel-glass ig_3 for the indicated temperatures. $\nu_{MAS}$ = 10 kHz; $\pi$/2-pulse lengths = 4.25 $\mu$s ($^{19}$F), 10 $\mu$s ($^{1}$H), 3.5 $\mu$s ($^{7}$Li); repetition time: 5−20 s ($^{19}$F), 30−60 s ($^{1}$H), 15 s ($^{7}$Li). Exponential line broadening of 10 Hz ($^{19}$F), 1 Hz ($^{1}$H), 5 Hz ($^{7}$Li) was used to smooth the data.

nonaqueous sol−gel route.[22] 1-Butyl-3-methylimidazolium tetrafluoroborate ([BMIM]$BF_4$, Aldrich) was used as the ionic liquid. In a typical synthesis procedure, 1 g of LiTf was dissolved in 4 mL of formic acid (HCOOH). To this, 2.7 mL of tetraethoxysilane (TEOS, Aldrich) was added (see Table 1 for the resulting molar ratios); the resulting mixture was stirred at room temperature for 10 min, during which a clear solution was formed. Upon addition of [BMIM]$BF_4$, gelation occurred within less than 1 min. Without the addition of the ionic liquid, the gelation took about 1 h. The clear and transparent gels were subsequently dried at 50 °C overnight and then stored at 110 °C for several weeks, resulting in transparent glass monoliths.

**NMR Experiments.** NMR measurements were carried out on a BRUKER DSX 400 spectrometer with resonance frequencies of 100.6, 155.5, 376.6, and 400.13 MHz for $^{13}$C, $^{7}$Li, $^{19}$F, and $^{1}$H, respectively, and on a Tecmag Apollo spectrometer operating at 7.04 T for $^{29}$Si (59.6 MHz). Spectra are referenced to 1 M aqueous LiCl for $^{7}$Li NMR, $CFCl_3$ for $^{19}$F NMR, adamantane [$\delta(CH_2)$ = 38.5 ppm] for $^{13}$C, and tetramethylsilane for $^{29}$Si and $^{1}$H. For the PFG NMR measurements, a commercial probe (Bruker Diff 30) was employed, which allows magnetic field gradients of up to 12 T/m. The self-diffusion coefficients were determined using the stimulated echo (PGSTE) technique.[23,24] The spectral width was set to 100 kHz ($^{1}$H, $^{13}$C) and 150 kHz ($^{7}$Li, $^{19}$F). More experimental details for the individual experiments are given in the figure captions.

(20) Neouze, M. A.; Le Bideau, J.; Gaveau, P.; Bellayer, S.; Vioux, A. *Chem. Mater.* **2006**, *18*, 3931.
(21) Le Bideau, J.; Gaveau, P.; Bellayer, S.; Neouze, M. A.; Vioux, A. *Phys. Chem. Chem. Phys.* **2007**, *9*, 5419.
(22) Sharp, K. G. *J. Sol−Gel Sci. Technol.* **1994**, *2*, 35.
(23) Stejskal, E. O.; Tanner, J. E. *J. Chem. Phys.* **1965**, *42*, 288.
(24) Price, W. S. *Concepts Magn. Reson.* **1997**, *9*, 299.

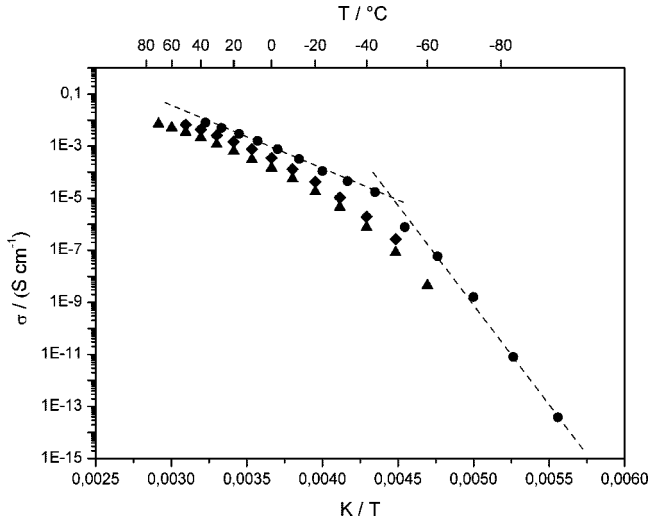


**Figure 5.** Ionic conductivity as a function of the inverse temperature for ionogel-glasses ig_2 (triangles), ig_3 (circles), and ig_3.2 (squares). For ig_3, an Arrhenius type of temperature dependence is observed at high ($T > 240$ K) and low ($T < 220$ K) temperatures with activation energies of 44 and 150 kJ mol$^{-1}$, respectively.

**Impedance Data.** Impedance data were acquired using a Novocontrol Alpha analyzer, which was connected to a BDS 1200 sample cell (Novocontrol). The sample material itself was prepared in a home-built sample chamber (stainless steel) to protect the sample from moisture. Data were collected in the frequency range from 10 mHz to 3 MHz with an ac voltage of 20 mV. Experiments were performed in the temperature range 180−320 K in steps of 10 K, employing stainless steel electrodes.

## Results and Discussion

The compositions of the ionogel-glasses studied in this work are compiled in Table 1. Annealing of the ionogel-glasses at 383 K for several days results in transparent and colorless glass monoliths. In the $^{29}$Si-MAS NMR spectra for the $SiO_2$/[BMIM]$BF_4$/LiTf ionogel-glasses (cf. Figure 1a) only a single resonance at −110 ppm can be identified, whereas in an ionic liquid-free reference sample $SiO_2$/LiTf, three different signals at −91, −101, and −111 ppm are discernible (cf. Figure 1b). The signals can be assigned to $Q^2$ (−91 ppm), $Q^3$ (−101 ppm), and $Q^4$ units (−110 ppm), employing the well-established $Q^n$ notation, in which $Q^n$ denotes a $SiO_4$ group connected to $n$ further $SiO_4$ tetrahedra. Thus, it seems that the addition of the ionic liquid considerably accelerates the condensation reactions, entailing a fully condensed glass network (i.e., complete gel-to-glass conversion) for the annealed samples, whereas for the IL-free samples, processed under identical conditions, the gel-to-glass conversion proves to be quite incomplete, producing a loose silicate network with a high residual amount of terminal Si−OH and Si−$OC_2H_5$ groups, in accord with the observations by Karout and Pierre.[25] In the $^1$H and $^{13}$C MAS NMR spectra for sample ig_3, which are collected in Figure 2 together with the corresponding spectra of pristine [BMIM]$BF_4$, no signals related to formic acid or ethanol can be identified, supporting the view of a fully condensed, solvent-free silica host confining the [BMIM]$BF_4$/LiTf mixture.

(25) Karout, A.; Pierre, A. C. *Catal. Commun.* **2009**, *10*, 359.

The dynamics of the ionic liquid and the Li salt within the pore system of the confining rigid silica network was analyzed by employing solid-state $^{19}$F and $^7$Li NMR techniques. The corresponding spectra are compiled in Figure 3 the spectra for pristine LiTf and for pristine [BMIM]$BF_4$ are incorporated for reference. The $^{19}$F-MAS and $^7$Li MAS NMR spectra for pristine LiTf (cf. Figure 3a,b) bear the typical characteristics for immobile triflate anions and Li cations with the observed numerous spinning sidebands indicating nonaveraged chemical shift anisotropy [$^{19}$F: $\delta_{iso} = -79.3$ ppm; $\Delta\sigma = 70$ ppm; $\Delta\sigma = \sigma_{33} - 0.5(\sigma_{11}+\sigma_{22})$] and quadrupole ($^7$Li, $C_Q = 65$ kHz) interactions; the width of the $m = 1/2 \rightarrow m = -1/2$ transition in the static $^7$Li NMR spectrum (Figure 2c; fwhm = 4.1 kHz) can be traced back to nonaveraged homo- and heteronuclear dipolar interactions. Upon incorporation of the ionic liquid and the LiTf into the $SiO_2$ matrix, distinctive changes in the appearance of the NMR spectra can be observed. Contrasted to the spectra for pristine LiTf, the number and intensity of the spinning sidebands in the $^7$Li MAS NMR spectra as well as the line width of the signal in the static $^7$Li NMR spectra are found to be drastically reduced. The reduction of the line width of the static $^7$Li NMR signal originates in an averaging of the homo- and heteronuclear dipolar interactions due to motional narrowing; the almost complete loss in spinning sideband intensity in the $^7$Li MAS NMR spectra indicates an averaging of the quadrupolar coupling of the $^7$Li nuclei, again due to the dynamics of the Li cations. A close inspection of the line widths and residual spinning sideband intensities discloses gradual changes in the Li mobility within the ionogel-glasses. Both parameters, the residual spinning sideband intensities and the static $^7$Li NMR line width (cf. Table 1), exhibit a decrease with increasing [BMIM]$BF_4$/LiTf ratio, thus indicating a corresponding increase in Li mobility. This increase in the mobility with increasing [BMIM]$BF_4$/LiTf ratio is also borne out by the $^{19}$F-MAS NMR spectra. Whereas for sample ig_1 the majority of the triflate anions remains immobile with the corresponding signal resembling that of pristine LiTf ($\delta_{iso} = -79.3$ ppm; $\Delta\sigma = 60 \pm 5$ ppm), the $^{19}$F-MAS NMR spectra for samples ig_2 and ig_3 display a single narrow signal at −79.3 ppm with only marginal spinning sideband intensity, suggesting high triflate mobility within the pore system of the $SiO_2$ network in these samples (Figure 3). Contrasted to this, the $BF_4$ anions (from the ionic liquid) are found to be mobile within the $SiO_2$ network, irrespective of the [BMIM]$BF_4$/LiTf ratio. For the corresponding signal (cf. Figure 2a), only two spinning sidebands of rather minor intensity can be observed for all studied ionogel-glasses. Nevertheless, the same principal trend as for the $^7$Li MAS NMR signal and the $^{19}$F MAS NMR signal of the triflate anions, a decrease in the spinning sideband intensity with increasing [BMIM]$BF_4$/LiTf ratio, is followed by this signal. Interestingly, the isotropic position of the $BF_4$ signal experiences a shift to higher field with decreasing [BMIM]$BF_4$/LiTf ratio. Thus, according to the solid-state NMR results, in the ionogel-glass samples with high [BMIM]$BF_4$ ratio (sample ig_3), the Li cations, triflate anions, $BF_4$ anions, and [BMIM] cations (as evidenced from the $^1$H MAS NMR spectra and $^{13}$C MAS NMR spectra, cf.

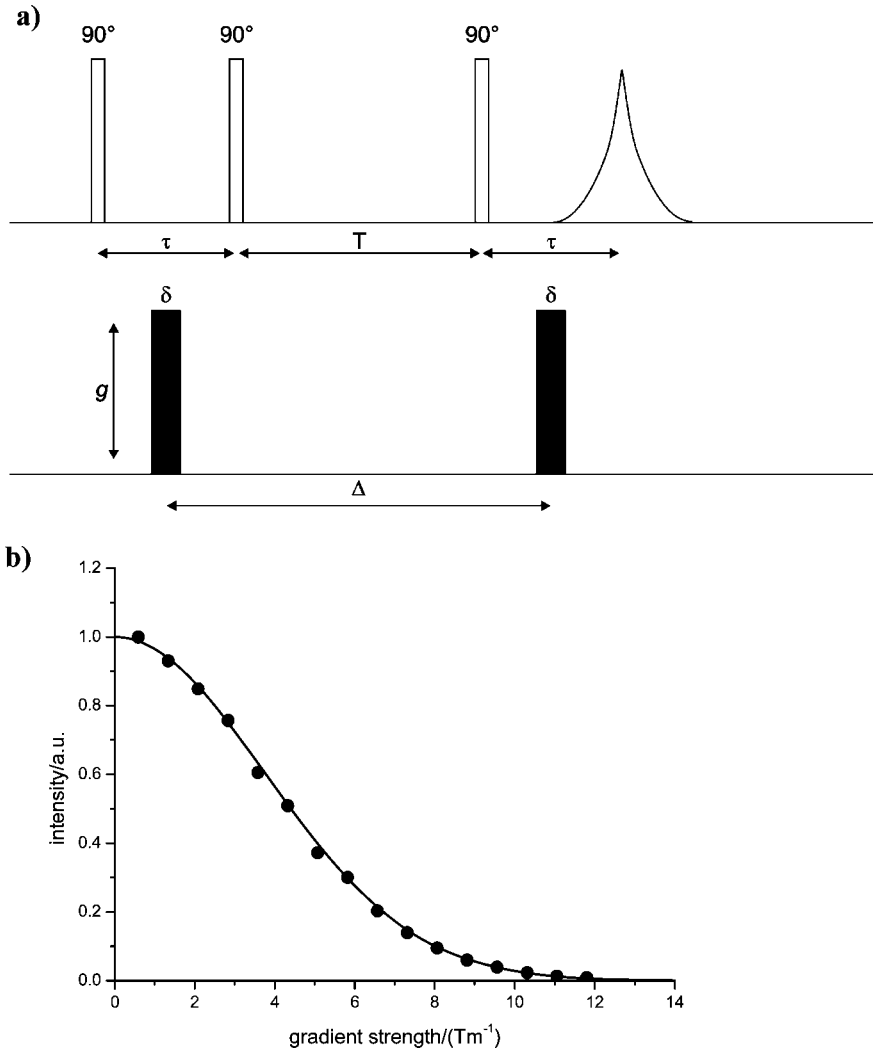


**Figure 6.** (a) Stimulated echo pulse sequence used for the PFG NMR experiments. The commercial PFG probe allows gradient strengths ($g$) of up to 11.8 T/m. (b) Results of a $^1$H PFG NMR experiment employing the pulse sequence in part a for sample [BMIM]$BF_4$/LiTf. The intensity of the stimulated echo is plotted as a function of the gradient strength $g$. Experimental details: $\delta = 1.5$ ms; $\Delta = 50$ ms; $\pi/2$ pulse length $= 4.5$ $\mu$s; $\tau = 3.7$ ms; relaxation delay $= 6$ s; line broadening $= 0.3$ Hz; spectral width $= 20\,000$ Hz. From the decay, the self-diffusion coefficient $D$ is obtained by fitting the decay to $I_{(g)} = I_{(0)} \exp[-D\gamma^2 g^2 \delta^2(\Delta - \delta/3]$.

**Table 2. Room Temperature Diffusion Coefficients (from PFG NMR) and Ionic Conductivities (from impedance spectroscopy) for the Samples Investigated in This Work**[a]

| | diffusion coefficients $D$ /($10^{-12}$ m$^2$s$^{-1}$) | | | | ionic conductivity $\sigma$ ($10^{-4}$ S cm$^{-1}$) | | | | |
|---|---|---|---|---|---|---|---|---|---|
| | | | | | calculated from $D$ for individual ions | | | | from impedance spectroscopy |
| sample | [BMIM]$^+$ | $Li^+$ | $Tf^-$ | $BF_4^-$ | [BMIM]$^+$ | $Li^+$ | $Tf^-$ | $BF_4^-$ | |
| [BMIM]$BF_4$ | 11 | – | – | 11 | – | – | – | – | – |
| [BMIM]$BF_4$/LiTf | 4.5 | 1.5 | 1.9 | 2.5 | – | – | – | – | – |
| ig_2 | – | 0.5 | 0.8 | 0.9 | – | – | – | – | 6.3 |
| ig_3[b] | 4.5 | 1.3 | 2.8 | 3.6 | 15 | 1.1 | 2.3 | 12 | 30 |
| ig_3.2[b] | 2.4 | 0.7 | 1.2 | 1.4 | 8 | 0.6 | 1.1 | 5 | 15 |

[a] The individual contributions to the total ionic conductivity were calculated from the diffusion coefficients employing $\sigma = \sum_{ion} \sigma^{ion} \propto \sum_{ion} x^{ion} D^{ion}$. [b] Repeated batches of the same compositions gave somewhat different absolute values for the ionic conductivity and the diffusion coefficients (cf. samples ig_3 and ig_3.2). This, however does not affect the observed overall dependence of these values on the [BMIM]$BF_4$/LiTf ratio.

Figure 2) are performing an almost liquidlike dynamic within the pore system of the fully condensed $SiO_2$ network. However, the presence of minor spinning sideband intensity in the $^1$H, $^{19}$F, and $^7$Li MAS NMR spectra indicates some restriction of the dynamics due to the confinement of the ionic liquid/LiTf within the pores of the $SiO_2$ network.

The perpetuation of the high Li mobility down to subambient temperatures constitutes a prerequisite for a good Li ion conductor for use in battery applications. This was confirmed by temperature-dependent $^{19}$F MAS, $^1$H, and $^7$Li NMR on sample ig_3. The corresponding spectra (cf. Figure 4) convincingly prove that the mobility of the cations ([BMIM]$^+$, $Li^+$) and anions (triflate, $BF_4^-$) extends down to a temperature of 240 K. Below this temperature, the distinct line broadening in the $^1$H and $^7$Li NMR spectra and the appearance of considerable spinning sideband intensity in the $^{19}$F MAS NMR spectra indicate a freezing of the motion of the various ionic species present in the system.

The established very high ionic mobility extending to temperatures down to 240 K in an albeit solid-state electrolyte system will only translate into good macroscopic ionic conductivity if the hosting $SiO_2$ matrix provides a connected pore system. Le Bideau and Vioux reported a conductivity of $\approx 10^{-3}$ S cm$^{-1}$ at ambient temperature in related, LiTf-free ionogel-glasses, from which the presence of a connected pore system, enabling macroscopic transport, could be concluded.[16] The ionic conductivities of the samples investigated in this work were determined from temperature-dependent impedance spectroscopy (cf. Figure 5). Again, the sample with the highest [BMIM]$BF_4$/LiTf ratio exhibits the best performance; a value of $0.5 \times 10^{-2}$ S cm$^{-1}$ at 300 K is observed. The temperature dependence of the conductivity at high and low temperatures follows an Arrhenius behavior with resulting activation energies of $E_A = 44 \pm 4$ kJ mol$^{-1}$ at high temperatures and $E_A = 150 \pm 4$ kJ mol$^{-1}$ at low temperatures with a change over at $T = 226$ K, i.e., roughly the same temperature at which the cation and anion dynamics is frozen (cf. Figure 3). The main interest in these samples, however, is not related to their overall ionic conductivity but to the Li ion conductivity. Since from the results of the impedance measurements it is not possible to separate the contributions from the various ions from one another, additional pulsed field gradient NMR experiments were performed. With PFG NMR the mobility of the various cations and anions present in the solid electrolytes can be studied individually via an evaluation of the respective diffusion coefficients. Thus, $^1$H, $^7$Li, and $^{19}$F PFG NMR experiments were performed to obtain the diffusion coefficients for [BMIM]$^+$ ($^1$H), $BF_4^-$ ($^{19}$F), $Li^+$ ($^7$Li), and triflate ($^{19}$F). The pulse sequence employed and a representative $^1$H-PFG NMR data set for [BMIM]$BF_4$/LiTf are given in Figure 6, the results are compiled in Table 2. The diffusion coefficients for pristine [BMIM]$BF_4$ and a [BMIM]$BF_4$/LiTf mixture (ratio 4:1, corresponding to ig_3) were determined as references. According to our results, the mobility of the [BMIM]$^+$ cation and $BF_4^-$ anion decreases by a factor of 2 and 4, respectively, upon addition of LiTf. Within this mixture, the Li cations, although representing the smallest ions in the system, exhibit the lowest diffusion coefficient, followed by Tf and $BF_4$, whereas [BMIM], constituting the largest ion, shows the highest diffusion coefficient. Interestingly, the confinement of the [BMIM]$BF_4$/LiTf mixture into the pore system of the silica glass (sample ig_3) does not entail a further deterioration of the ionic mobility. Rather, the diffusion coefficients are found to be more or less identical to those of the mixture. Again, the mobility is found to scale with the inverse of the ion size, in accordance with published data for various binary ionic liquid/lithium salt systems.[26,27] As outlined in ref 27, this indicates that whereas the larger [BMIM] cation diffuses as a single ion, neither the $TF^-$ and $BF_4^-$ anions nor the Li cations diffuse as single ions, but rather are involved in the formation of temporary lithium−anion complexes, which also explains the observed stronger effect of salt addition on the anion mobility. (cf. Table 2). A rough estimate for the Li conductivity in the samples—ignoring any correlation effects such as ion pairing or the formation of larger anion−cation agglomerates—may be calculated from the diffusion coefficients obtained from PFG NMR using $\sigma = \sum_{ion} \sigma^{ion} \propto \sum_{ion} x^{ion} D^{ion}$. The obtained individual ionic conductivities are incorporated in Table 2. As expected, the ions from the ionic liquid provide the dominant contribution to the total ionic conductivity; nonetheless, the ionic conductivity obtained for the Li cations ($1.1 \times 10^{-4}$ S cm$^{-1}$ at ambient temperature) presents an encouraging high value for a solid Li ion conductor.

## Conclusions

To conclude, the high ionic conductivity that extents down to subambient temperatures in combination with the high mechanical stability of the fully condensed $SiO_2$ network renders this class of material a particular promising prospect for a solid electrolyte for battery applications. Owing to the large degree of chemical flexibility (variation of the glass matrix, the ionic liquid, and the Li salt), further improvement of the material may be anticipated in the near future.

**Acknowledgment.** Financial support by the Deutsche Forschungsgemeinschaft (SFB 458) is gratefully acknowledged.

CM9005184

(26) Hayamizu, K.; Aihara, Y.; Nakagawa, H.; Nukuda, T.; Price, W. S. *J. Phys. Chem. B* **2004**, *108*, 19527.
(27) Monteiro, M. J.; Bazito, F. F. C.; Siqueira, L. J. A.; Ribeiro, M. C. C.; Torresi, R. M. *J. Phys. Chem. B* **2008**, *112*, 2102.